Presence of a Richardson's regime in kinematic simulations

F. C. G. A. Nicolleau* and A. F. Nowakowski

Sheffield Fluid Mechanics Group, Department of Mechanical Engineering, The University of Sheffield, Sheffield, United Kingdom

(Received 7 June 2010; revised manuscript received 14 March 2011; published 16 May 2011)

In this paper we investigate kinematic simulation (KS) consistency with the theory of Richardson [Proc. Roy. Soc. A **110**, 24 (1926)] for two-particle diffusivity. In particular we revisit the sweeping problem. It has been argued by Thomson and Devenish [J. Fluid Mech. **526**, 277 (2005).] that due to the lack of sweeping of small scales by large scales in kinematic simulation, the validity of Richardson's power law might be affected. Here, we argue that the discrepancies between authors on the ability of kinematic simulation to predict Richardson power law may be linked to the inertial subrange they have used. For small inertial subranges, KS is efficient and the significance of the sweeping can be ignored, as a result we limit the KS agreement with the Richardson scaling law t^3 for inertial subranges $k_N/k_1 \leqslant 10000$. For larger inertial range KS does not fully follow the t^3 law. Unfortunately, there is no experimental data to compare KS with and draw conclusions for such large inertial subranges. It cannot be concluded either that the discrepancy between KS and Richardson's theory for larger inertial subranges is exactly taken into account by the theory developed in Thomson and Devenish [J. Fluid Mech. **526**, 277 (2005).].

DOI: 10.1103/PhysRevE.83.056317 PACS number(s): 47.27.E−, 47.27.tb

I. INTRODUCTION

A. The two-particle dispersion problem

The two-particle separation is defined as

$$\Delta(t) = |\mathbf{X}_2(t) - \mathbf{X}_1(t)|, \tag{1}$$

where $\mathbf{X}_1(t)$ is the position of the first particle and $\mathbf{X}_2(t)$ the position of the second particle at time t. The first quantity of interest is the mean-square separation between the two particles $\langle\Delta^2(t)\rangle$ as a function of time which has received much research attention since the pioneering work of [1] (see, e.g., [2–14]).

It is worth noting that the reference work in [1] refers to the diffusivity $(d/dt)\langle\Delta^2(t)\rangle$ as a function of the mean-square separation, $\langle\Delta^2(t)\rangle$, for two particles in the inertial subrange of turbulence, that is, for particle pairs such that $\eta < \Delta(t) < L$, where L is the upper limit length scale of the inertial range or integral scale and η the lower limit or Kolmogorov scale. Richardson introduced the locality assumption and derived his four-third law of diffusion,

$$\frac{d}{dt}\langle\Delta^2(t)\rangle \sim \Delta^{\frac{4}{3}}(t). \tag{2}$$

His locality assumption states that the mean-square separation reaches a limit as the averaging time is increased because only eddies comparable in size with the separation are effective in further statistical increase of the mean-square separation.

From Eq. (2), neglecting the initial separations Δ_0 and applying Kolmogorov's similarity theory to the relative diffusion of particles, [15] and [16] obtained the famous t^3 law for the diffusion in isotropic turbulence and in the inertial range of times:

$$\langle\Delta^2(t)\rangle = G_\Delta \epsilon t^3, \tag{3}$$

where G_Δ is the Richardson universal dimensionless constant and ϵ the rate of energy dissipation per unit mass.

B. Observation of the Richardson law

Since Richardson derived his formula for the particle relative diffusion there has been much endeavor to verify it. However, experimental measurements of Lagrangian statistics and validation of the power law (3) are not straightforward. This comes from the problem of tracking the positions of particle pairs at the very large frequencies required in high Reynolds number flows. Laboratory experiments [17,18] report observations of Richardson scaling in two-dimensional and three-dimensional flows for Reynolds numbers Re_λ up to 104.

Numerical simulations [19–22] also struggle to achieve sufficiently large Reynolds numbers owing to the high computational demands required to solve the Navier-Stokes equations. [14] concluded that DNS with Reynolds numbers large enough to observe (3) and measure directly the constant G_Δ are not possible in the near future and we can only, for the time being, rely on extrapolations from the present Reynolds numbers (see also [23] for a review of Richardson's validation).

This is something to bear in mind when assessing kinematic simulation's ability to reproduce (3) at large Reynolds numbers. KS can give prediction for particles' Lagrangian statistics at large Reynolds numbers but to our knowledge there are no experimental data to compare with for inertial scale ranges of 10^4 or larger.

C. Kinematic simulation's predictions

Many studies have been done using KS to understand the turbulent diffusion of particle pairs. This has been done either to validate the power law in different ranges of Reynolds numbers or to find a specific value for the Richardson constant, G_Δ, which still has uncertainties in its value. There have been some contradictory conclusions as to the ability of KS to predict a t^3 law. According to [5,6,9,12] KS predicts (2); according to [2] it does not. The main argument against KS to be found in this latter reference [2] is that

*F.Nicolleau@Sheffield.ac.uk

"A consequence of the way the flow is constructed is that, in contrast to real turbulence, there is no sweeping of the smaller eddies by the larger eddies."

In this paper, we limit our study to the classical KS for isotropic flows without a mean velocity. For this case Ref. [2] predicted that

"The separation process then follows t^6 in the bulk of the flow but follows Richardson's classical t^3 law in regions where the velocity is much smaller than the r.m.s. velocity. [...] Because of the way the size of these regions varies in time, the resulting mean-square separation grows like $t^{9/2}$."

In the present work, we study particle pair separations in an isotropic turbulent flow using KS and investigate the ability of this method to reproduce the well-known Richardson's law. The numerical approach used to generate the turbulent flow field is introduced in Sec. II; the results obtained are presented in Sec. III. We generalize the approach to energy distribution different from the classical $-5/3$ power spectrum in Sec. IV and examine the effect of the KS unsteadiness parameter in Sec. V. Conclusions are summarized in Sec. VI.

II. KINEMATIC SIMULATION TECHNIQUE

Kinematic simulation is a particular case of synthetic turbulence. By synthetic turbulence we mean handmade analytical flows which spare one the need to fully solve Navier-Stokes equations. Synthetic turbulence has been used as an approach to understand the general mechanisms of turbulent diffusion, and also to make quantitative predictions of relative dispersion and higher order Lagrangian statistical moments. A simple model should capture the essence of the physics. Such is the idea with synthetic turbulence which retains less information than the whole flow, but try to keep what is paramount for the Lagrangian statistics.

Synthetic turbulence began to emerge with [24] (see also [25–27]), in which diffusion was simulated on a one-dimensional grid with a random velocity field. Reference [28] continued with a random flow field in three dimensions, and constructed incompressible fields as an isotropically random sum of unsteady Fourier modes. These were the basis for the kinematic simulation developed in [3,29]. These models are not intended as a simulation of the Eulerian field, but only of the Lagrangian statistics that would arise from such synthesized underlying Eulerian fields. This Eulerian field is only intended to be a qualitatively accurate representation of an actual turbulent field, which contains certain important flow structures in an qualitative way. This kind of computation does not require the storage of a lot of data with very big tables as with direct numerical simulation.

In [6] KS were compared to the direct numerical simulation (DNS) results of [19]. It was found that KS did exhibit Richardson's scaling and also reproduced the large flatness in the relative velocity observed in DNS. This was important as the relative velocity flatness is a measure of Lagrangian intermittency and this supported the idea that relative diffusion happens in sudden bursts when an appropriate flow structure is encountered. Here lies one of the most important aspects of kinematic simulation, the incorporation of flow structure, upon which the relative diffusion and higher order statistics depend.

A. The KS method for isotropic turbulence

In kinematic simulation the underlying Eulerian velocity field is generated as a sum of random incompressible Fourier modes with a prescribed energy spectrum. The computational simplicity of KS allows one to consider large inertial subranges and Reynolds numbers Re. With this method, the computational task reduces to the calculation of the trajectory of each particle placed in the turbulent field, each trajectory is, for a given initial condition, solution of the differential equation:

$$\frac{d\mathbf{x}}{dt} = \mathbf{u}_E(\mathbf{x},t), \tag{4}$$

where $\mathbf{u}_E$ is the analytical Eulerian velocity used in KS. In this paper, as in [5,30], it takes the form of a truncated Fourier series, sum of N_k random Fourier modes:

$$\mathbf{u}(\mathbf{x},t) = \sum_{n=0}^{N_k} \mathbf{a_n}\cos(\mathbf{k_n}\cdot\mathbf{x} + \omega_n t) + \mathbf{b_n}\sin(\mathbf{k_n}\cdot\mathbf{x} + \omega_n t), \tag{5}$$

where $\mathbf{a_n}$ and $\mathbf{b_n}$ are decomposition coefficients corresponding to the wave vector $\mathbf{k_n}$, and ω_n is the unsteadiness frequency.

The wave vectors $\mathbf{k_n} = k_n\hat{\mathbf{k}}_\mathbf{n}$ are oriented randomly by ensuring that the unit vectors $\hat{\mathbf{k}}_\mathbf{n}$ have a random, uniformly distributed, orientation. The magnitude of the wave numbers included in the summation can be given an arbitrary distribution. Usually they are decimated so as to reduce computational demands, while including enough modes for the convergence of the Lagrangian statistics. Reference [31] tried arithmetic, geometrical, and linear distributions and found that the distribution,

$$k_n = k_1\left(\frac{k_{N_k}}{k_1}\right)^{(n-1)/(N_k-1)}, \tag{6}$$

where n is an integer satisfying $1 \leqslant n \leqslant N_k$, gives the fastest convergence of the statistics.

The coefficient vectors $\mathbf{a_n}$ and $\mathbf{b_n}$ are chosen randomly and independently in the plane normal to $\mathbf{k_n}$,

$$\mathbf{a_n}\cdot\mathbf{k_n} = \mathbf{b_n}\cdot\mathbf{k_n} = 0, \tag{7}$$

to ensure that the random field is incompressible. In order to impose an energy spectrum, $E(k)$ upon the field, the magnitudes of the coefficients are chosen as follows:

$$|\mathbf{a_n}|^2 = |\mathbf{b_n}|^2 = 2E(k_n)\Delta k_n, \tag{8}$$

where

$$\Delta k_n = \frac{k_{n+1} - k_{n-1}}{2}. \tag{9}$$

The spectrum used usually follows the universal form in the inertial range,

$$E(k) = C_k\epsilon^{2/3}k^{-5/3}, \tag{10}$$

where C_k is the Kolmogorov constant ($C_k = 1.5$) and ε is the dissipation rate of energy per unit mass, but departures from this scaling have also been studied, partly for intermittency corrections but also to try to gauge the importance of the energy spectrum scaling on the Lagrangian statistics in kinematic simulation. In this study, we will use an energy spectrum

characterized by a power law with an exponent, p, varying from 1.15 to 1.96:

$$E(k_n) \sim u_{\rm rms}^2 L\,(k_n L)^{-p} \quad \text{for} \quad k_1 \leqslant k_n \leqslant k_N, \tag{11}$$

where we have introduced the rms of the turbulent velocity fluctuation,

$$u_{\rm rms} = \sqrt{\frac{2}{3}\int_{k_1}^{k_N} E(k_n)dk}, \tag{12}$$

and the integral length scale of the isotropic turbulence is defined as follows:

$$L = \frac{3\pi}{4}\frac{\int_{k_1}^{k_N} k^{-1}E(k_n)dk}{\int_{k_1}^{k_N} E(k_n)dk}. \tag{13}$$

The Kolmogorov length scale is defined as $\eta = 2\pi/k_N$. The ratio between the integral and Kolmogorov length scales is $L/\eta = k_N/k_1$ which is used to determine the inertial range and the associated Reynolds number: ${\rm Re} = (L/\eta)^{4/3} = (k_N/k_1)^{4/3}$. A characteristic time for normalization is introduced as $t_d = L/u_{\rm rms}$.

B. The Eulerian field time dependence

A time dependence of the velocity field can be incorporated through the unsteadiness frequency ω_n. This is often taken as the eddy turnover time of the $n^{\rm th}$ mode,

$$\omega_n = \lambda\sqrt{k_n^3 E(k_n)}. \tag{14}$$

A wide range of values of the parameter λ has been studied, from near-frozen fields to extremely unsteady fields. It has been shown [6] that in three-dimensional isotropic KS for two-particle diffusion, most of the statistical properties are insensitive to the unsteadiness parameter's value, provided that it rests in the range $0 \leqslant \lambda \leqslant 1$.

The interactions between the random Fourier modes are not modeled as such in KS, hence KS misses their dynamics. As a result the small eddies are not advected by the large ones, a KS shortcoming called "lack of sweeping" between different modes. Recently Ref. [2] has proposed that the second-order statistics in kinematic simulation are dominated by this absence of sweeping. They have investigated the particle pair separation using KS paying a particular attention to this problem. As a consequence of the lack of sweeping, it is expected that the two-particle mean-square separation will be different from Richardson's scaling because the large scales in real life do influence the rate of separation. Reference [2] predicted that in the absence of sweeping, the variance of the particle separation should increase as $t^{9/2}$. This was confirmed by their KS results for two inertial subranges $k_N/k_1 = 10^6$ and 10^8.

However, Ref. [32] has investigated the separation of particle pairs using kinematic simulation for inertial subrange in the range $k_N/k_1 = 10^4$ and concluded that KS reproduces Richardson's power law over their range of scales. This was also consistent with the results in Ref. [12].

TABLE I. Different cases studied for two-particle diffusivity, $u_{\rm rms} = 1$, $L = 1$, $p = 5/3$, and $\Delta_0/\eta = 10$.

Case	$\frac{k_N}{k_1}$	λ	η	Case	$\frac{k_N}{k_1}$	λ	η
A	10^3	0	6.28×10^{-3}	J	10^4	1	6.28×10^{-4}
F	10^4	0	6.28×10^{-4}	N	10^5	0	6.28×10^{-5}
G	10^4	0.25	6.28×10^{-4}	S	10^6	0	6.28×10^{-6}
H	10^4	0.5	6.28×10^{-4}	T	10^6	0.5	6.28×10^{-6}
I	10^4	0.75	6.28×10^{-4}	U	10^6	1	6.28×10^{-6}

III. RICHARDSON REGIME AND KS INERTIAL RANGE

A. Varying the inertial range

To clarify these apparent contradictory conclusions, it is worth reporting from the main studies cited here the inertial subrange which was used for the particle diffusion. In [5] the two-particle diffusion was investigated using a two-dimensional KS and Richardson's law was observed on an inertial subrange $k_N/k_1 = 4000$.

In [9], three-dimensional KS was used to determine the relation between the generalized Richardson's power law exponent for the pair separation, γ, and the fractal dimension of the stagnation points, D_s. The inertial range used was $k_N/k_1 = 1000$. The results showed remarkable consistency between the KS predictions and the generalization of Richardson's theory for different values of the energy spectrum exponent $1 \leqslant p \leqslant 2$.

In [12], two-particle diffusion in a three-dimensional KS was studied for different power law exponents of the energy spectrum from 1.2 to 3. Richardson's prediction was again verified in the limited range $k_N/k_1 = 2000$ provided that the initial pair separation was larger than the Kolmogorov length scale.

We can conclude from this partial survey that KS studies using inertial ranges k_N/k_1 up to 4000 yield results in agreement with Richardson's prediction, whereas Ref. [2] results questioning this agreement were obtained for a much larger range up to 10^8.

In this section we present KS made for the full range $10^3 \leqslant k_N/k_1 \leqslant 10^6$, in order to study the effect of the Reynolds number. We fix the initial separation to be $\Delta_0/\eta = 10$ to make a direct comparison with the results obtained in [2]. All the runs' parameters are tabulated in Table I for an rms velocity $u_{\rm rms} = 1$ m s^{-1} and an integral length scale $L = 1$ m. The statistics were performed over 4000 realizations of the flow field.

B. Particle pair diffusivity for $p = 5/3$:

In Fig. 1, the particle pair separation $\langle\Delta^2\rangle/L$ is plotted as a function of time for different inertial subranges, $10^3 \leqslant k_N/k_1 \leqslant 10^6$. The slope of Richardson's scaling (t^3) and the slope proposed in [2] ($t^{9/2}$) are added to the figure. It can be noticed that for small inertial subranges, up to $k_N/k_1 = 10^4$, the curves seem to follow Richardson's scaling t^3, but for higher inertial ranges they seem rather to follow the scaling $t^{9/2}$. As mentioned in Sec. I, for [1] the reference quantity was

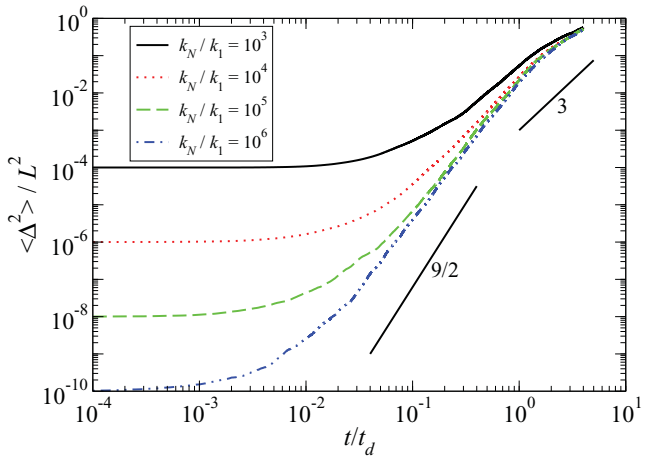

FIG. 1. (Color online) Two-particle separation as a function of time for different inertial subranges (cases A, F, N, and S in Table I).

the two-particle diffusivity. The locality in scale assumption was made for the diffusivity. Working directly on

$$\frac{d}{dt}\langle\Delta^2(t)\rangle \sim \langle\Delta^2(t)\rangle^{2/3} \tag{15}$$

is keeping closer to this fundamental assumption. Furthermore, Ref. [12] argued that plots of pair separations as functions of time as in Fig. 1 can be misleading and their analysis needs to be complemented by an analysis in terms of diffusivity. In particular, conclusions are easier to draw from plots of $(d/dt)\langle\Delta^2(t)\rangle$ as they remove part of the initial separation (Δ_0) effects.

Accordingly, we compute directly the diffusivity by differentiating $\langle\Delta^2(t)\rangle$. In Fig. 2(a) we plot the compensated diffusivity,

$$\frac{d}{dt}\langle\Delta^2\rangle/\langle\Delta^2\rangle^{2/3}, \tag{16}$$

as a function of $\langle\Delta^2\rangle/L^2$ for the different cases of Fig. 1, whereas, for comparison in Fig. 2(b) we plot $(d/dt\langle\Delta^2\rangle)/\langle\Delta^2\rangle^{7/9}$ as a function of $\langle\Delta^2\rangle/L^2$ for the same cases. A horizontal trend will validate each law, respectively. There are two other well-known regimes which are worth mentioning: the Batchelor regime at small times t, where $\langle\Delta^2\rangle \sim \Delta_0^2 + V_0^2 t^2$, and the diffusive regime where $\langle\Delta^2\rangle \sim t$ for large times. The diffusive regime is clearly identified by the dashed line having the corresponding slope in Figs. 2(a) and 2(b). The advantage of the plots we use is that the small time and small separation regimes are squeezed with respect to the large diffusivity regimes (those in the inertial range

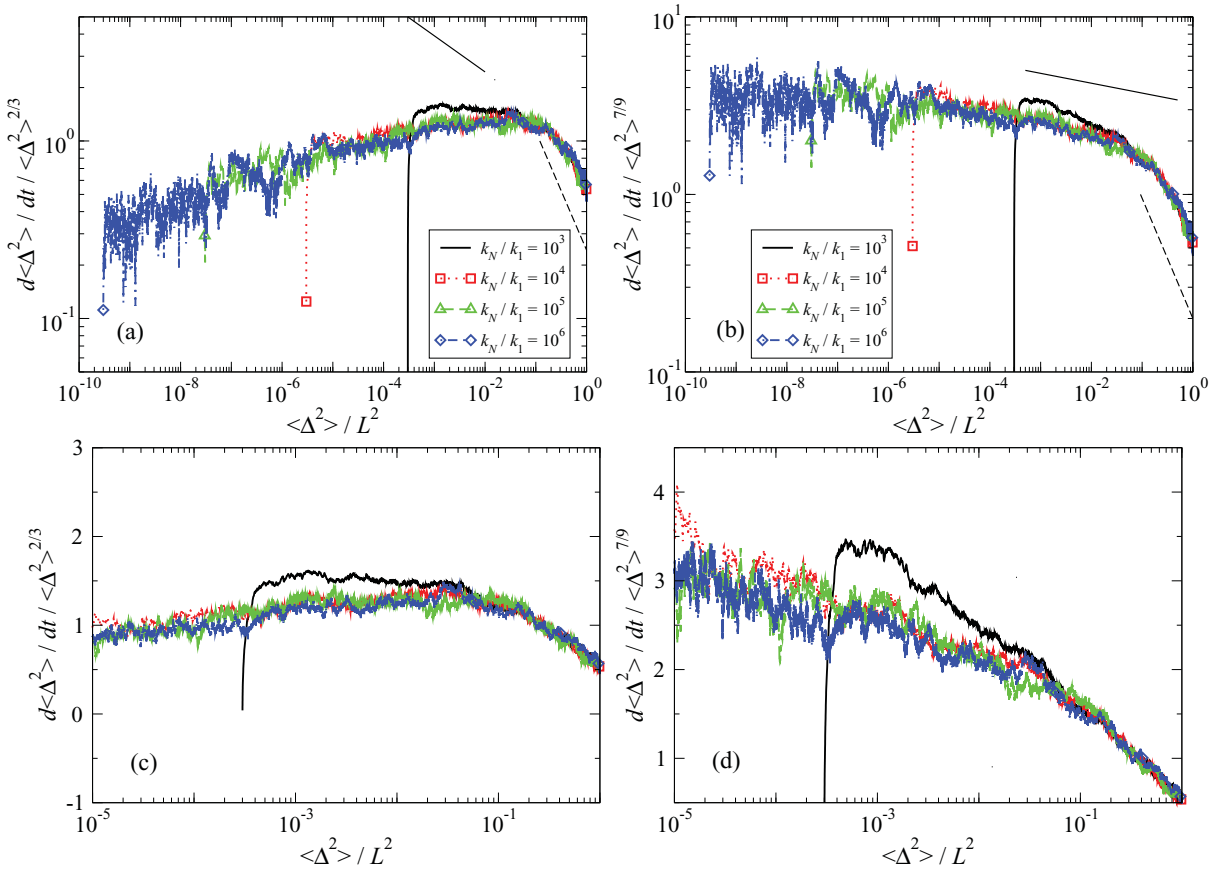

FIG. 2. (Color online) Compensated diffusivity, for the cases in Fig. 1, $p = 5/3$. (a) $(d/dt)\langle\Delta^2\rangle/\langle\Delta^2\rangle^{2/3}$ as a function of Δ^2/L^2; (b) $(d/dt\langle\Delta^2\rangle)/\langle\Delta^2\rangle^{7/9}$ as a function of $\langle\Delta^2\rangle/L^2$; the dashed line corresponds to the large time t regime and the solid line to the Batchelor t^2 regime; (c) magnification of plot (a) around the Richardson range with a linear scale along the y axis; (d) magnification of plot (b) for the same range of scales with a linear scale along the y axis.

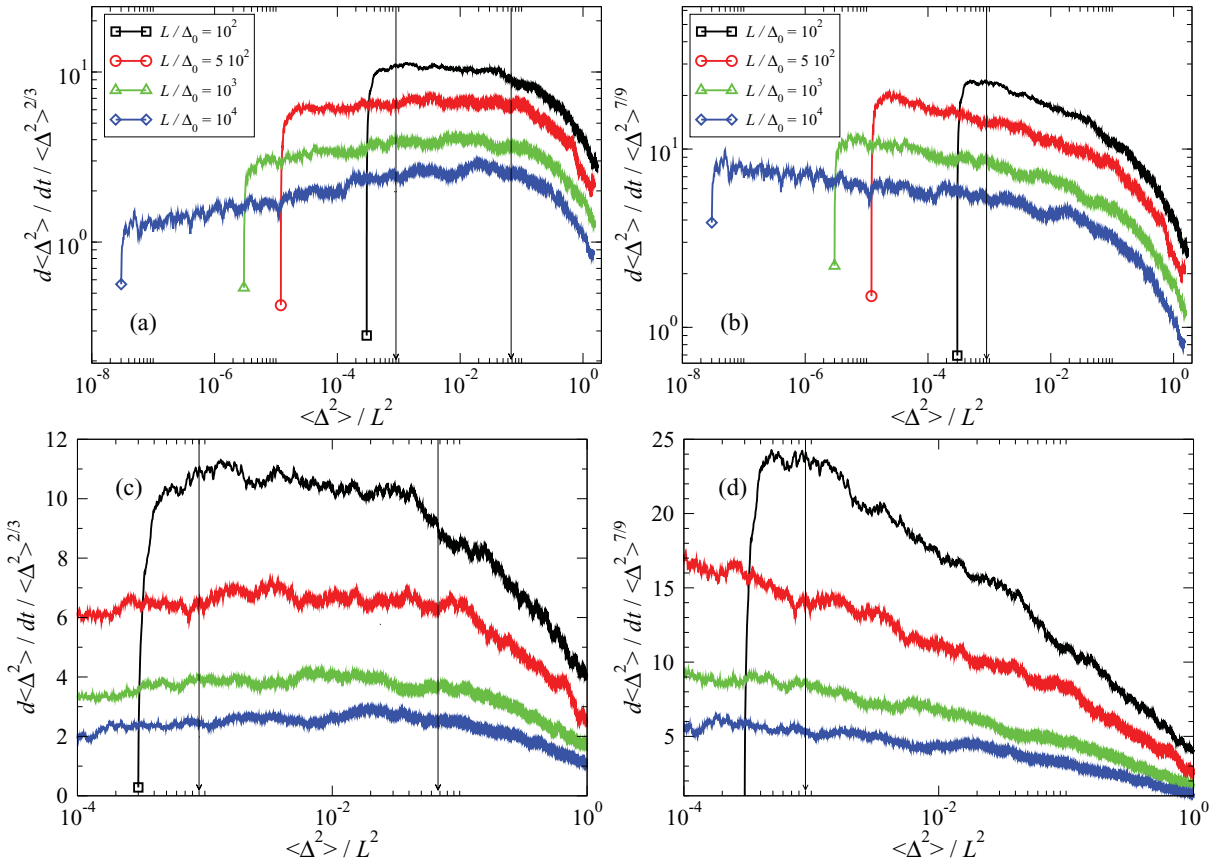

FIG. 3. (Color online) Compensated diffusivity as a function of $\langle\Delta\rangle^2/L^2$ for different initial separations (cases G, J, L, and M in Table II). (a) $d/dt\langle\Delta^2\rangle/\langle\Delta^2\rangle^{2/3}$, (b) $d/dt\langle\Delta^2\rangle/\langle\Delta^2\rangle^{7/9}$, (c) same as (a) with a linear scale on the y axis, (d) same as (b) with a linear scale on the y axis.

of scales). This is confirmed in Fig. 2 where the diffusivity exhibits a constant slope down to the smallest scales, that is, the Batchelor regime cannot be seen in such plots; for the sake of completeness we add the solid line corresponding to a t^2 regime.

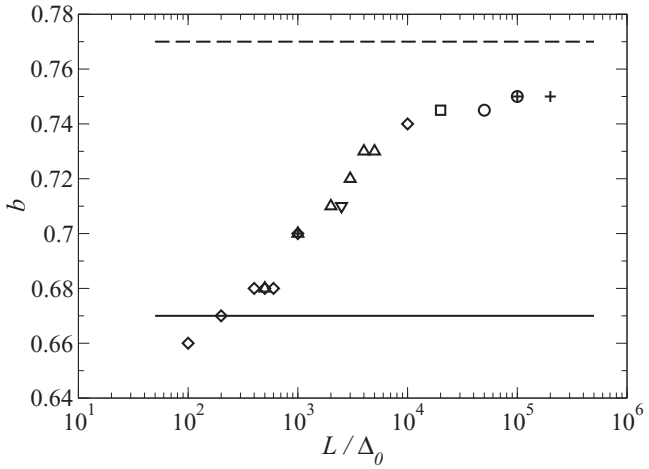

FIG. 4. Power law exponent from Eq. (16) as a function of L/Δ_0 for cases in Table II. The dashed line corresponds to the Thomson and Devenish prediction, the plain line to Richardson's value 2/3. Symbols correspond to different Δ_0/η, namely (cross) $\Delta_0/\eta = 1$, (circle) $\Delta_0/\eta = 2$, (square) $\Delta_0/\eta = 5$, (diamond) $\Delta_0/\eta = 10$, (up-triangle) $\Delta_0/\eta = 20$, and (down-triangle) $\Delta_0/\eta = 40$.

Comparing Figs. 2(a) and 2(b) we can conclude as suggested by [32] that neither law are satisfactorily observed over the entire inertial range of scales. More precisely,

$$\frac{d}{dt}\langle\Delta^2\rangle \sim \langle\Delta^2\rangle^{2/3} \tag{17}$$

seems to be observed for inertial ranges $k_N/k_1 \leqslant 10^4$ only. For larger ranges, Eq. (17) is verified only after large separations [i.e., when $\Delta/L \geqslant 100$ as can be seen in Fig. 2(c)]. Otherwise, for the inertial ranges $k_N/k_1 > 10^4$ and $\Delta/L < 100$, comparisons of Figs. 2(a) and 2(b) indicate that the diffusivity is closer to $\langle\Delta^2\rangle^{7/9}$ than to $\langle\Delta^2\rangle^{2/3}$ but the power dependence is not 7/9 which appears clearly as an overestimation, except perhaps for the range $3\times10^{-10} < \langle r^2\rangle/L^2 < 3\times10^{-6}$ for $L/\Delta_0 > 10^5$; the exact value reported later on in Fig. 4 is 0.75.

To clarify this behavior in Fig. 3(a) we plot the compensated diffusivity (16) as a function of $\langle\Delta^2\rangle/L^2$ for four different ratios Δ_0/L, namely 0.01, 0.005, 0.001, and 0.0001, cases G, J, L, and M in Table II. The different curves have been arbitrarily translated along the y axis to have a clearer view of the two ranges. The two vertical arrows point toward the range of scales where a Richardson law is observed, that is,

$$0.03 < \frac{\sqrt{\langle\Delta^2\rangle}}{L} < 0.26. \tag{18}$$

TABLE II. In all cases $\lambda = 0$, $p = 5/3$, the number of realizations is larger than 3000, and $\eta = 2\pi$.

Case	$\frac{L}{\Delta_0}$	$\frac{\Delta_0}{\eta}$	$\frac{k_N}{k_1}$	Case	$\frac{L}{\Delta_0}$	$\frac{\Delta_0}{\eta}$	$\frac{k_N}{k_1}$	Case	$\frac{L}{\Delta_0}$	$\frac{\Delta_0}{\eta}$	$\frac{k_N}{k_1}$
A	10^3	1	10^3	G	10^2	10	10^3	N	5×10^2	20	10^4
B	10^5	1	10^5	H	2×10^2	10	2×10^3	O	10^3	20	2×10^4
C	2×10^5	1	2×10^5	I	4×10^2	10	4×10^3	P	2×10^3	20	4×10^4
D	5×10^4	2	10^5	J	5×10^2	10	5×10^3	Q	3×10^3	20	6×10^4
E	10^5	2	2×10^5	K	6×10^2	10	6×10^3	R	4×10^3	20	8×10^4
F	2×10^4	5	10^5	L	10^3	10	10^4	S	5×10^3	20	10^5
				M	10^4	10	10^5	T	2.5×10^3	40	10^5

That range is independent of L/Δ_0 provided that $L/\Delta_0 > 100$. It persists when L/Δ_0 increases so it is not an effect of small inertial range. For smaller ranges the determination of a power law cannot be conclusive. This corresponds to $L/\Delta_0 < 10^2$ in our KS as illustrated in Figs. 2 and 3. This is the minimum range needed to observe the plateau we identified at large scales. Figure 3 indicates that this plateau is then fixed for $L/\Delta_0 \geqslant 5 \times 10^2$. However, most DNS would correspond to such small ranges, so for the sake of comparison we show results down to $L/\Delta_0 = 10^2$ in Fig. 4.

Before that large-scale range (when $\langle\Delta^2\rangle/L^2 < 10^{-4}$), the law followed by the diffusivity depends on the initial separation, more exactly on the ratio L/Δ_0 and departs more and more from Richardson's prediction. We will see in the next section that eventually it reaches an asymptote in between 2/3 and 7/9. In other words, Fig. 3 shows that KS seems to struggle with Richardson's locality-in-scales hypothesis at small scales but follows that hypothesis for larger scales. For the sake of comparison we plot the same diffusivity compensated by $\langle\Delta^2\rangle^{7/9}$, the figure shows clearly that there is no region where that scaling is observed. However, the scaling seems to get closer to 7/9 when L/Δ_0 increases.

C. Estimation of the diffusivity power law at small scales

In order to quantify better the power law dependence on the initial separation L/Δ_0 we run many different cases with different ratios L/Δ_0 and Δ_0/η. These different cases are reported in Table II. For each case we plot

$$\frac{d}{dt}\langle\Delta^2\rangle/\langle\Delta^2\rangle^b, \tag{19}$$

as a function of Δ^2/L^2, tuning the coefficient b in order to find the best power law describing the diffusivity before the range (18) where Richardson's prediction is observed. The values for b as a function of L/Δ_0 are reported in Fig. 4. The two horizontal lines correspond to Richardson's prediction (2/3) and to the Ref. [2] prediction (7/9).

The general trend confirms our previous observation, that is, for small L/Δ_0, b is close to Richardson's prediction. It then starts to depart significantly from that prediction around $L/\Delta_0 = 1000$ to come closer to the 7/9 prediction. It becomes closer to that prediction than to Richardson's for $L/\Delta_0 > 3000$. It then levels off for $L/\Delta_0 > 3 \times 10^4$ around a value of b in the range $[0.74; 0.75]$. That is slightly short of the Ref. [2] prediction. Computing cost prevented us from investigating larger inertial ranges but the asymptote of the curve seems clearly below 7/9. We estimate the error in the slope measurements to be smaller than ± 0.01, in most cases smaller than ± 0.005. We also varied the ratio Δ_0/η (see Table II) and find no effect of this parameter confirming that the main parameter is L/Δ_0, that is, the portion of the inertial range that is seen by the particle pair (provided, of course, that $\Delta_0/\eta \geqslant 1$).

IV. SENSITIVITY TO THE ENERGY SPECTRUM POWER LAW

A. Generalization of diffusivity formula

The difference between the Richardson and the Ref. [2] predictions, respectively, 0.67 and 0.78 is certainly significant but it remains a difference of just about 16%. Furthermore, we have seen that larger scales seem to follow Richardson's theory.

It is therefore important to support our work with a generalization to a range of spectral power laws to look for a general trend or isolate $p = 5/3$ as a peculiar case. the effect of the energy spectrum power law on the diffusivity was introduced in [33] and [34]. Generalizing [1] it is assumed that the diffusivity depends only on the spectrum $E(k)$ and a wave number k_Δ which is of the order of $\sqrt{\langle\Delta^2\rangle}$ so that

$$\frac{d}{dt}\langle\Delta^2\rangle = f\{E(k_\Delta), k_\Delta\}, \tag{20}$$

with $k_\Delta \sim \sqrt{\langle\Delta^2\rangle}$. Using dimensional arguments, the diffusivity must be of the form,

$$\frac{d}{dt}\langle\Delta^2(t) \sim \langle\Delta^2\rangle^{1/4}\sqrt{E(\sqrt{\langle\Delta^2\rangle})}. \tag{21}$$

Equation (15) can then be written in a general form for a turbulence energy spectrum (11) as follows:

$$\frac{d}{dt}\langle\Delta^2(t)\rangle \sim u_{\rm rms} L\left(\frac{\langle\Delta^2(t)\rangle}{L^2}\right)^c, \tag{22}$$

with $c = \frac{1+p}{4}$, which leads to

$$\langle\Delta^2(t)\rangle \sim L^2\left(t\frac{u_{\rm rms}}{L}\right)^{\frac{1}{1-c}}, \tag{23}$$

with $\frac{1}{1-c} = \frac{4}{3-p}$. The characteristic time associated with the pair is defined as

$$\tau \sim \frac{L}{u_{\rm rms}}\left(\frac{\langle\Delta^2(t)\rangle}{L^2}\right)^{\frac{3-p}{4}}, \tag{24}$$

TABLE III. Different cases studied for two-particle separations, for different power spectra; $\Delta_0/\eta = 10$ for all cases.

Case	$\frac{k_N}{k_1}$	p	λ	η	Case	$\frac{k_N}{k_1}$	p	λ	η
					N	10^6	1.15	0	6.28×10^{-6}
B	10^4	1.27	0	6.28×10^{-4}	O	10^6	1.27	0	6.28×10^{-6}
C	10^4	1.37	0	6.28×10^{-4}	P	10^6	1.37	0	6.28×10^{-6}
D	10^4	1.47	0	6.28×10^{-4}	Q	10^6	1.47	0	6.28×10^{-6}
E	10^4	1.57	0	6.28×10^{-4}	R	10^6	1.57	0	6.28×10^{-6}
					S	10^6	1.62	0	6.28×10^{-6}
					T	10^6	1.70	0	6.28×10^{-6}
K	10^4	1.77	0	6.28×10^{-4}	V	10^6	1.77	0	6.28×10^{-6}
L	10^4	1.87	0	6.28×10^{-4}	W	10^6	1.87	0	6.28×10^{-6}
M	10^4	1.96	0	6.28×10^{-4}	X	10^6	1.96	0	6.28×10^{-6}

where p is the energy spectrum exponent and varies as $1 \leqslant p \leqslant 2$. When $E(k) \sim k^{-5/3}$ we retrieve $c = 2/3$ and $\langle \Delta^2 \rangle \sim t^3$. Equation (22) is more general but still relies on Richardson's locality-in-scale hypothesis.

B. KS prediction for $E(k) \sim k^{-p}$

In order to see the consistency of KS with this hypothesis and to have a better idea of the effect of increasing the inertial subrange on the KS prediction of Richardson's law, we repeat the previous results for different spectral power laws. We vary p in Eq. (11) from 1.15 to 1.96 and also vary the inertial range k_N/k_1 (see the different cases reported in Table III).

Figure 5 shows $(d\langle \Delta^2 \rangle/dt)/\langle \Delta^2 \rangle^c$ as a function of $\langle \Delta^2 \rangle/L^2$ where c is given by Eq. (22) for the different spectral power laws and an inertial range $k_N/k_1 = 10^4$. For easier interpretation we plot the cases $p < 5/3$ in Fig. 5(a) and the cases $p > 5/3$ in Fig. 5(b). The results are consistent with what was observed for the case $p = 5/3$ (i.e., all the curves show a remarkable consistency of KS with Richardson's locality-in-scale hypothesis and the prediction in Refs. [5,33] (22) for the same small range $\sqrt{\langle \Delta \rangle^2}/L$ given in (18). For smaller $\sqrt{\langle \Delta \rangle^2}/L$, similarly to the case $p = 5/3$, the diffusivity departs from the generalization of Richardson power law in Refs. [5,33].

When comparing Figs. 3 and 5 we can conclude that the locality-in-scale hypothesis and Eq. (22) are verified for $1.15 \leqslant p \leqslant 1.96$ over the same range of scales $\sqrt{\langle \Delta^2 \rangle}/L$ (18). This generalizes the conclusion made for $p = 5/3$ that KS is remarkably consistent with the locality assumption as it shows this agreement for the different values of p. The KS difficulty to match Richardson's prediction can therefore be localized to small scales and there is no effect of the spectral power law p on this range.

C. Generalization of Thomson and Devenish sweeping effect to $E(k) \sim k^{-p}$

The argument of [2] on the effect of sweeping can be generalized to any spectral law. We follow the simplified approach of [32] here: The eddy diffusivity as the rate of the particles' mean-square separation can be expressed in terms of a characteristic relative velocity ΔV between fluid element pairs and a time scale τ over which such relative velocities change.

$$\frac{d}{dt}\langle \Delta^2(t) \rangle \sim \Delta V^2 \tau. \tag{25}$$

Both ΔV and τ are functions of the mean-square separation $\langle \Delta^2(t) \rangle$. The relative velocity is given by the spectral law as follows for a structure of characteristic size r:

$$\Delta V \sim \sqrt{E(k)\Delta k} \sim u_{\rm rms} \left(\frac{L}{r}\right)^{\frac{1-p}{2}}, \tag{26}$$

and τ is given by

$$\tau(\langle \Delta^2(t) \rangle, u') \sim \min\left(\frac{\sqrt{\langle \Delta^2(t) \rangle}}{u'}, \frac{L}{u_{\rm rms}}\left(\frac{\sqrt{\langle \Delta^2(t) \rangle}}{L}\right)^{\frac{3-p}{2}}\right). \tag{27}$$

Reference [2] introduces mean-square separations conditional on u', that is, $\langle \Delta^2 \rangle_{u'}$, so that

$$\langle \Delta^2 \rangle = \int_0^\infty \langle \Delta^2 \rangle_{u'}\, p(u') du', \tag{28}$$

where $p(u')$ is the probability density function associated with the turbulence velocity u'. There are two regimes:

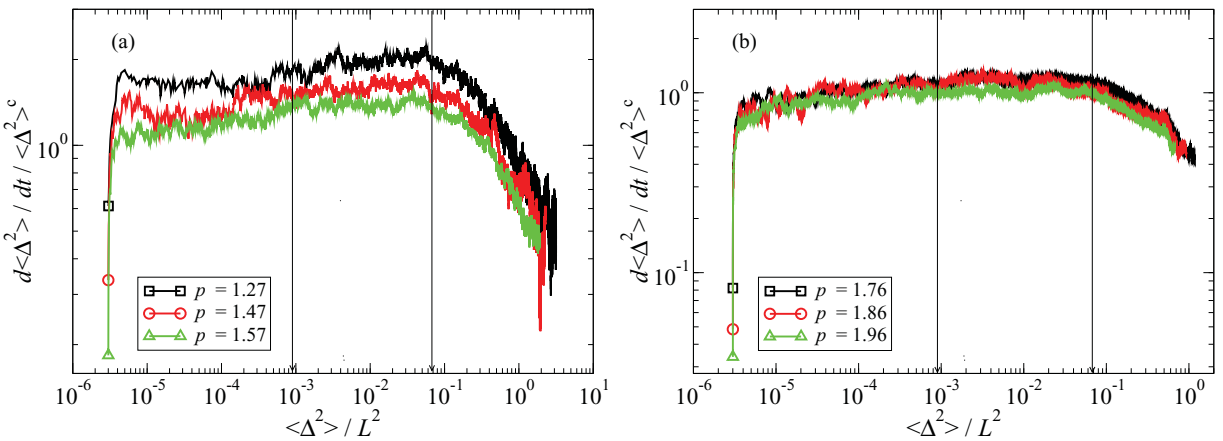

FIG. 5. (Color online) $(d\langle \Delta^2 \rangle/dt)/\langle \Delta^2 \rangle^c$ as a function of $\langle \Delta^2 \rangle/L^2$ for different energy spectrum power laws and $k_N/k_1 = 10^4$ (cases B, C, D, E, F, K, L, and M in Table I).

(1) According to the assumption in Ref. [2] when u' is small enough the sweeping problem is absent and (23) applies, therefore $\langle\Delta^2(t)\rangle \sim L^2\,(t\frac{u_{\rm rms}}{L})^{\frac{4}{3-p}}$, that is, for $p = 5/3$ $\langle\Delta^2\rangle_{u'} \sim \epsilon t^3$.

(2) Whereas, when u' is large enough, we start from (25) which becomes

$$\frac{d}{dt}\langle\Delta^2(t)\rangle \sim u_{\rm rms}^2\frac{L}{u'}\left(\frac{\langle\Delta^2(t)\rangle}{L^2}\right)^{\frac{p}{2}}. \tag{29}$$

$\langle\Delta^2\rangle_{u'}$ is sweeping dominated so that

$$\langle\Delta^2\rangle_{u'} \sim L^2\left(\frac{u_{\rm rms}^2}{u'L}t\right)^{\frac{2}{2-p}}, \tag{30}$$

that is, for $p = 5/3$ $\langle\Delta^2\rangle_{u'} \sim \epsilon^4 t^6/u'^6$.

The separation which divides these two regimes can be estimated as $L^2\,(t\frac{u_{\rm rms}}{L})^{\frac{4}{3-p}} \sim L^2(\frac{u_{\rm rms}^2}{u'L}t)^{\frac{2}{2-p}}$, that is,

$$u'_{\rm sep} \sim \left(\frac{t u_{\rm rms}^{\frac{2}{p-1}}}{L}\right)^{\frac{p-1}{3-p}}, \tag{31}$$

which corresponds to $u' \sim \sqrt{\epsilon t}$ for $p = 5/3$.

$$\langle\Delta^2\rangle_{u'} \sim \int_0^{u'_{\rm sep}} L^2\,\left(t\frac{u_{\rm rms}}{L}\right)^{\frac{4}{3-p}} p(u')du' + \int_{u'_{\rm sep}}^{\infty} L^2\left(\frac{u_{\rm rms}^2}{u'L}t\right)^{\frac{2}{2-p}} p(u')du'. \tag{32}$$

We use for u' the pdf proposed in [2]:

$$p(u') = \sqrt{\frac{2}{\pi}}\frac{u'^2}{u_{\rm rms}^3}e^{-\frac{1}{2}\frac{u'^2}{u_{\rm rms}^2}}, \tag{33}$$

and obtain

$$\langle\Delta^2\rangle \sim L^2\left(t\frac{u_{\rm rms}}{L}\right)^{\frac{3p+1}{3-p}}, \tag{34}$$

which leads to results in Ref. [2] for $p = 5/3$. The expression for the diffusivity is obtained by differentiating (34)

$$\frac{d}{dt}\langle\Delta^2(t)\rangle \sim u_{\rm rms}L\left(\frac{\langle\Delta^2(t)\rangle}{L^2}\right)^{\frac{4p-2}{3p+1}}. \tag{35}$$

In Fig. 6(a) we compare the results from KS to the two predictions (23) from [5,33] and (35) from the generalization of the Ref. [2] argument. The points in Fig. 6(a) are the results from KS. Similarly to the case $p = 5/3$ reported in Fig. 4, for $p \neq 5/3$, when $L/\Delta_0 \geqslant 10^5$ results do not change. We measured c outside the range of scales for which Morel and Larchevêque is observed. It is measured for an inertial range $L/\Delta_0 \geqslant 10^5$ large enough for it to have reached its asymptotic value. It is neither Morel and Larchevêque nor the extension of 7/9 which is observed but the intermediary value c that we are reporting, which is clearly above the Ref. [5,33] prediction and below the generalization of the Ref. [2] theory.

The departure from the theory in Refs. [5,33] increases up to $p = 5/3$ and then levels off around a value $c = 0.77$, very close to 0.75, the limit value for $p = 2$.

Figure 6(b) shows the relative error of the two theories when compared to the KS values. Interestingly, the maximum discrepancy between KS and the theory in Refs. [5,33] is

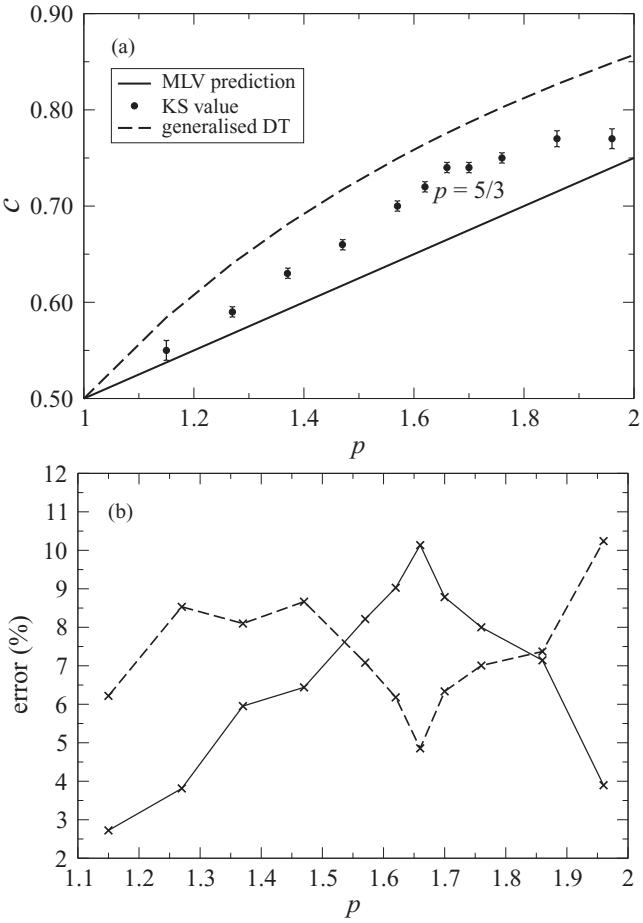

FIG. 6. Power c from Eq. (22). (a) (Solid line) Theoretical value (23) as predicted by Morel and Larchevêque, (points) results from KS, (dashed line) value as predicted from (35); (b) relative error in % between the power c measured from KS and the values from (23) (solid line) and (35) (dashed line). $k_N/k_1 = 10^6$ (cases N to X in Table III).

observed for the case $p = 5/3$ where the Ref. [2] theory gives a better prediction of the KS result. Apart from that range around $p = 5/3$, KS results are very close to the predictions in Refs. [5,33]. It is worth noting that the generalization of [2] converges to predictions for $p = 1$ and $p = 1$ from [5,33]. $p = 1$ corresponds to the lower limit of integrability for the energy spectrum. Such spectra would have a much more even distribution of energy than the classical 5/3. The largest discrepancy between the two theories occurs for $p = 1.775$. This value could be thought of as the point where the absence of sweeping is the most harmful to KS, however, as noted before KS departs the most significantly from [5,33] earlier at $p = 5/3$ where it gets closer to the generalisation of [2].

It is reasonable to believe that, approaching the two limiting cases $p = 1$ and $p = 3$, the lack of sweeping of the small eddies becomes less relevant, for two opposite reasons.

As p gets closer to 1, the energy spectrum becomes flatter, the characteristic velocity is more or less the same over the range of scales modeled by KS so that a sweeping of small eddies by large eddies loses its relevance as indicated by the convergence of both theories to the same prediction $c = 0.5$.

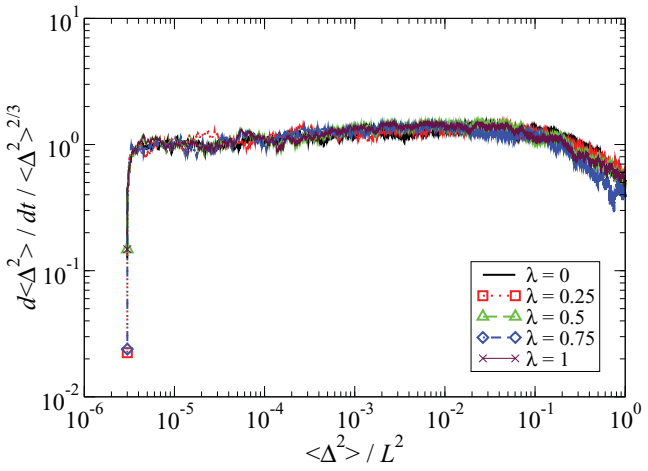

FIG. 7. (Color online) Effect of the unsteadiness parameter on the normalized diffusivity with respect to Richardson's law as a function of the two-particle separations, $p = 5/3$ and $k_N/k_1 = 10^4$ (cases F, G, H, I, and J in Table I).

Similarly for $p \to 3$ both theories converge to $c = 1$. In this case the energy spectrum tends to a very sharp distribution on the large scales. The particle advection is completely dominated by the large scales in the flow. The contribution of the small eddies where KS struggles with Richardson's locality assumption becomes less important. Therefore the accurate modeling of their sweeping by large scales is not so important anymore. This is supported by our observation that KS follows remarkably Richardson's locality assumption at large scales.

Overall KS seems more consistent with the generalization in Refs. [5,33] of Richardson's hypothesis to $p \neq 5/3$ than expected from a generalization of the Ref. [2] approach.

V. EFFECT OF VARYING THE UNSTEADINESS PARAMETER ON THE VALIDITY OF RICHARDSON REGIME

It is worth remembering that sweeping mechanisms have been proposed for KS; the most popular is the term ω_n defined in Eq. (14). In all the cases we studied before, the unsteadiness parameter λ was fixed to 0 as there is no conclusive result from previous researches showing it has any significative effect in three-dimensional KS.

In order to show if this parameter has an effect on KS prediction of Richardson law, we repeat our results for $p = 5/3$ for $0 \leqslant \lambda < 1$. Figure 7 shows the results for $k_N/k_1 = 10^4$ corresponding to cases F, G, H, I, and J in Table I. From that figure it can be noticed that λ has no effect on the prediction of the diffusivity scaling. We repeated the results for $k_N/k_1 = 10^6$ (not shown here) and did not find any effect of λ either.

VI. CONCLUSION

Questions were raised about the applicability of the kinematic simulation approach to the separation of pairs in real turbulent flows, in particular, because of their inability to model accurately the sweeping of small eddies by large eddies.

We can conclude from our study that KS is consistent with Richardson's prediction for turbulence with inertial ranges up to $k_N/k_1 < 10^4$. That may be enough for practical applications of KS as a subgrid, for instance. This would already correspond to very high actual engineering Reynolds numbers.

The problem remains: KS prediction departs from the Ref. [33] prediction at small scales for large inertial ranges. However, our results are still close to the theoretical prediction and it would be fairer to conclude that the KS prediction is not as good at small separation than at large separation. It is perhaps premature to discard the KS prediction altogether for larger inertial range as there are no experimental results on such large ranges we can rely on for comparison.

Furthermore, if we accept the sweeping problem as it is used in [2] we can conclude that it does not seem to have much effect at larger scales where KS follows remarkably Richardson's theory as extended to spectral power laws $1.15 \leqslant p \leqslant 1.96$ (Refs. [5,33] prediction) and limited effects at small scales for $1 < p < 1.6$ and $1.7 < p < 2$.

ACKNOWLEDGMENTS

This work was supported by the Engineering and Physical Sciences Research Council through the UK Turbulence Consortium (Grant No. EP/G069581/1).

[1] L. F. Richardson, Proc. Roy. Soc. A **110**, 709 (1926).
[2] D. J. Thomson and B. J. Devenish, J. Fluid Mech. **526**, 277 (2005).
[3] F. W. Elliott and A. J. Majda, Phys. Fluids **8**, 1052 (1996).
[4] D. J. Thomson, J. Fluid Mech. **210**, 113 (1990).
[5] J. C. H. Fung and J. C. Vassilicos, Phys. Rev. E **57**, 1677 (1998).
[6] N. A. Malik and J. C. Vassilicos, Phys. Fluids **11**, 1572 (1999).
[7] P. Flohr and J. C. Vassilicos, J. Fluid Mech. **407**, 315 (2000).
[8] P. Castiglione and A. Pumir, Phys. Rev. E **64**, 056303 (2001).
[9] J. Davila and J. C. Vassilicos, Phys. Rev. Lett. **91**, 144501 (2003).
[10] F. Nicolleau and J. C. Vassilicos, Phys. Rev. Lett. **90**, 024503 (2003).
[11] S. Goto and J. C. Vassilicos, New J. Phys. **6**, 65 (2004).
[12] F. Nicolleau and G. Yu, Phys. Fluids **16**, 2309 (2004).
[13] A. ElMaihy and F. Nicolleau, Phys. Rev. E **71**, 046307 (2005).
[14] B. L. Sawford, P. K. Yeung, and J. F. Hackl, Phys. Fluids **20**, 065111 (2008).
[15] A. M. Obukhov, Izv. Akad, Nauk, Ser. Geogr. Geofiz. **5**, 453 (1941).
[16] G. K. Batchelor, Quart. J. R. Met. Soc. **76**, 133 (1950).
[17] M.-C. Jullien, J. Paret, and P. Tabeling, Phys. Rev. Lett. **82**, 2872 (1999).
[18] S. Ott and J. Mann, J. Fluid Mech. **422**, 207 (2000).
[19] P. K. Yeung, Phys. Fluids **6**, 3416 (1994).
[20] T. Ishihara and P. K. Yeung, Phys. Fluids **14**, L69 (2002).

[21] P. K. Yeung and M. S. Borgas, J. Fluid Mech. **503**, 93 (2004).
[22] M. S. Borgas and P. K. Yeung, J. Fluid Mech. **503**, 125 (2004).
[23] J. P. Salazar and L. R. Collins, Annu. Rev. Fluid Mech. **41**, 40532 (2009).
[24] J. M. Lumley, Adv. Geophys. **6**, 179 (1959).
[25] D. J. Thomson, Q. J. R. Meterol. Soc. **110**, 1107 (1984).
[26] H. van Dop, F. T. M. Nieuwstadt, and J. C. R. Hunt, Phys. Fluids **85**, 1639 (1985).
[27] B. L. Sawford, Phys. Fluids **29**, 3582 (1986).
[28] R. H. Kraichnan, Phys. Fluids **13**, 22 (1970).
[29] J. C. H. Fung, J. C. R. Hunt, N. A. Malik, and R. J. Perkins, J. Fluid Mech. **236**, 281 (1992).
[30] F. Nicolleau and A. ElMaihy, Phys. Rev. E **74**, 046302 (2006).
[31] S. Goto, D. R. Osborne, J. C. Vassilicos, and J. D. Haigh, Phys. Rev. E **71**, 015301(R) (2005).
[32] D. R. Osborne, J. C. Vassilicos, K. Sung, and J. D. Haigh, Phys. Rev. E **74**, 036309 (2006).
[33] P. Morel and M. Larchevêque, J. Atm. Sc. **31**, 2189 (1974).
[34] J. C. H. Fung, J. Geophys. Res. **103**, 27905 (1998).